ELSEVIER

Journal of Nuclear Materials 307–311 (2002) 111–115

journal of nuclear materials

www.elsevier.com/locate/jnucmat

Overview of fuel retention in composite and tungsten limiters

M. Rubel [a,*], V. Philipps [b], A. Pospieszczyk [b], T. Tanabe [c], S. Kötterl [d]

[a] *Alfvén Laboratory, Royal Institute of Technology, Association EURATOM-VR, Teknikringen 31, 100 44 Stockholm, Sweden*
[b] *Institute for Plasma Physics, Forschungszentrum Jülich, Association EURATOM, Trilateral Euregio Cluster (TEC), 52425 Jülich, Germany*
[c] *Centre for Integrated Research in Science and Engineering (CIRSE), Nagoya University, Chikusa-ku, Nagoya, 464 Japan*
[d] *Max-Planck-Institute für Plasma-Physik, Association EURATOM, 85748 Garching, Germany*

Abstract

A number of materials, in a form of limiters, have been tested at the TEXTOR tokamak as candidates for plasma facing components in future devices. The results for fuel distribution and content in sole tungsten and composites (vacuum plasma sprayed tungsten layer on graphite and a B_4C coating on copper) are reported and compared with earlier obtained results for sole tungsten and graphite. In sole tungsten the deuterium content is below 1×10^{15} cm^{-2}, whereas in case of the composite targets the inventory found in the hottest parts of the limiters is one at least order of magnitude greater. The fuel content on composites is predominantly related to the co-deposition process with carbon and boron. The influence of material damage (melting, detachment of a coating) and material mixing processes on the fuel retention is also addressed.

1. Introduction

Fuel retention in plasma facing components (PFC) predominantly derives from the local and global ion transport in the plasma edge [1,2]. The quantitative effects are strongly material [3] and temperature dependent [4]. Significant inventory of hydrogen isotopes measured in controlled fusion devices with the first wall made of graphite or carbon fibre composites (CFC) [1–6] is related to the carbon erosion [7,8] and consecutive co-deposition of eroded and transported species together with large quantities (even over 30 at.%) of hydrogen isotopes [1–6]. Therefore, the major challenge is to decrease the in-vessel fuel inventory and the corresponding level of radioactivity in case of D–T operation. This is a driving force stimulating studies of materials, other than carbon, as acceptable plasma facing materials (PFM). An application of the all molybdenum wall in Alcator C-Mod leads to a decreased fuel inventory [9] in comparison to that observed in carbon containing machines. Several long experimental campaigns were performed at ASDEX Upgrade with tungsten coated graphite tiles covering the divertor (coating thickness 500 μm) [10,11] and the central column (500 nm thick layer) [12]. Selection and testing of materials for next-step devices is also an important and strongly addressed point in the research programme carried out at the TEXTOR tokamak [13–16]. The aims of testing are: (i) to evaluate the impact of a candidate material on the plasma performance, (ii) to recognise the material erosion and damage, i.e. to assess its lifetime, (iii) to determine the fuel retention. In recent years experiments with some tens of various materials serving as limiters and various configurations of those limiters have been performed.

The intention of this work is to give a concise overview of fuel retention and material mixing processes occurring on limiters at TEXTOR. The results previously obtained for sole targets such as tungsten and graphite are compared with those for composites manufactured by vacuum plasma spraying (VPS): a tungsten coating on graphite and a B_4C layer (tetraboron carbide)

* Corresponding author. Tel.: +46-8 16 11 99/790 60 93; fax: +46-8 15 86 74/24 54 31.
E-mail address: rubel@fusion.kth.se (M. Rubel).

0022-3115/02/$ - see front matter
PII: S0022-3115(02)00940-6

on a thick copper substrate. The latter composite was tested at TEXTOR as a candidate for the first wall components of the Wendelstein-7X stellarator [17,18].

As already shown in the reported works, in graphite and CFC the retention is determined by a co-deposition process [1–6] whereas in case of sole tungsten (in areas free of carbon co-deposition), the inventory is mostly connected with a direct implantation of ions and neutrals [15]. However, the data regarding fuel inventory and material mixing on composites exposed to extreme power loads (of around 20 $W m^{-2}$) in tokamak experiments have been gathered for the first time.

2. Experimental procedure

TEXTOR is operated with graphite PFC heated to a base temperature of up to 350 °C. Plasma radius is defined by two major arrays of limiters moveable in radial direction: a belt toroidal (ALT II [19]) consisting of eight blades (total area of 3.4 m^2, i.e. approximately 9% of the first wall area) and a main poloidal composed of two sets, each of them containing five tiles (total area of 0.06 m^2). There is also an inner bumper limiter and rf antenna protection tiles. In addition, so-called test limiters of mushroom shape are used for studies dedicated to material erosion and transport.

For material testing reported in this paper all 10 graphite blocks of the poloidal array were replaced by tiles coated with sprayed tungsten [20]. In separate experiments, test limiter systems were used for the exposure of sole tungsten, graphite and B_4C coated copper. The test specimens were installed in the torus on special manipulators to allow the change of the radial position, the rotation and heating of the limiter heads [15,21]. Heating is indispensable for sole W targets in order to avoid their damage by thermal shocks, i.e. to maintain the limiters' temperature above the ductile-to-brittle transition temperature of about 450 °C. Basic characteristics and exposure conditions of specimens are briefly summarized in Table 1.

The exposed targets were retracted from the machine, transferred to a surface analysis station and then examined with a number of methods. The amount and distribution of deuterium and boron was determined by means of nuclear reaction analysis using a $^3He^+$ (0.7 and 1.5 MeV) and a H^+ beam (0.65 MeV), respectively. The information depth in D analysis on carbon substrates is around 1.2 μm with a 0.7 MeV beam and 4.5 μm at 1.5 MeV. In case of tungsten the depth is approximately 50% smaller. The content of other elements (e.g. W, Si, Cu) was examined with Rutherford backscattering spectroscopy, whereas enhanced proton scattering was applied for tracing the carbon deposit on tungsten surfaces. Scanning electron microscopy (SEM) combined with energy dispersive X-ray spectroscopy (EDS) allowed studies of topographical details and the composition of VPS-W coating before and after its exposure to the plasma.

3. Results and discussion

Results from various tokamaks reveal non-uniform distribution of retained fuel and co-deposited plasma impurity atoms on PFC [1,4–6,22]. In this sense, the results presented below are in line with that fact. However, we want to focus on material aspects. For that reason, in case of the VPS coated targets we have chosen to examine in detail tiles partly damaged by the plasma, i.e. with partly detached or melted coating. Such approach gives a good insight into morphological changes (structure and composition) induced by the plasma operation in various regions of the targets. First we describe the morphology of the VPS coated specimens and this is followed by the comparison with the results previously obtained for sole tungsten and graphite.

3.1. Tungsten coatings

Fig. 1 shows a poloidal limiter tile with the detached and partly melted VPS-W coating. The tile shown here was a component of the poloidal array placed in the bottom of the machine. Though the coating was detached it did remain on the underlying substrate. Both sides of the coating (plasma facing side and the one originally attached to graphite), re-crystallized pieces of W, the underlying graphite substrate and side surfaces (i.e. areas being in gaps between the tiles) of the block were analyzed as marked in Fig. 1(a). The other side of the tile (facing the ion drift direction) and a detached

Table 1
Material characteristic and exposure conditions of limiters at TEXTOR

Limiter material	Material characteristic	Type of limiter	Exposure time (s)	Surface T_{max} (K)
W	Sole metal	Test	Up to 600	>3600
VPS-W layer on EK98 graphite	500 μm coating with a W-Re sandwich interlayer as a diffusion barrier between W and C	Main poloidal	750	>3600
C	Graphite EK98	Test	Up to 600	>3000
VPS-B_4C layer on Cu	170 μm coating	Test	100	>2700

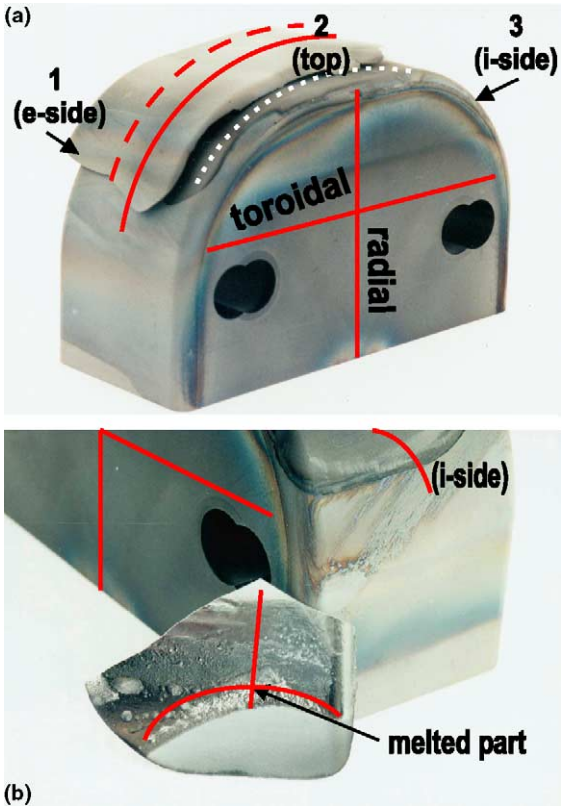

Fig. 1. A damaged tile of the poloidal limiter. Dimensions of the limiter block: projected length 120 mm (toroidal direction), width 50 mm (poloidal direction), height 78 mm. (a) The detached VPS-W coating and the graphite block. Lines of analysis on the coating and the graphite substrate are shown by dashed lines. (b) The view from the ion drift direction.

piece of tungsten with a molten zone are shown in Fig. 1(b). The presence of interference colours indicates the formation of co-deposits on all side surfaces, whereas the top part of the VPS-W coating remains shiny metallic suggesting less deposition. Detailed results for the content of trapped fuel and co-deposited atoms in those various regions on the top of the limiter are collected in Table 2. The amount of fuel is relatively small (10^{16}–10^{17}cm^{-2} range) but the results clearly indicate the retention on the VPS coating to be strongly influenced by co-deposition of deuterium with carbon, boron and eroded and promptly re-deposited tungsten. Because of material mixing process no definite clue as to the D trapping in the tungsten layer itself can be obtained.

Distribution of D and B on the side surface is plotted in Fig. 2. Equal amounts of species can be considered incidental. More important are their nearly identical radial profiles from which net erosion and net deposition zones are clearly distinguished. In the net deposition region the e-folding length (λ) can be determined: $\lambda_D = 17$ mm and $\lambda_B = 19$ mm. Besides of D and B there are also significant re-deposited and mixed species of carbon (not possible to determine quantitatively on the graphite substrate) and tungsten (over 10^{18} cm^{-2}). This indicates significant amounts of W being eroded from the VPS coating and transported to the side surfaces and also to the gaps between the tiles.

The damage to the coating will be discussed in a separate paper being under preparation. However, we want to mention that out of 10 tiles, two were seriously damaged by the plasma. The reason for the exfoliation could be related to some manufacturing failure but, certainly, also thermo-mechanical properties of the interlayer components are to be taken into account: (i) the mismatch between linear thermal expansion coefficients of graphite ($\alpha_C = 3.9 \times 10^{-6}$ K^{-1}) and rhenium ($\alpha_{Re} = 6.2 \times 10^{-6}$ K^{-1}) and (ii) the difference of melting temperatures between tungsten ($T_m = 3407$ °C) and rhenium ($T_m = 3180$ °C). These differences could play an important role in the destruction of the rhenium layer [23,24] when the power load to the limiter exceeded 20 MW m^{-2} causing the temperature rise above 3000 °C [20]. Such high and strongly localized power loads might also be the reason that the damage to the VPS-W coatings at TEXTOR was more severe than that

Table 2
Distribution and content of deuterium and other species in various areas of the VPS-W coated poloidal limiter

Area	D (10^{17} cm^{-2})	C (10^{17} cm^{-2})	B (10^{17} cm^{-2})
VPS coating (front side)			
e-side (1)	2.4–3.6	52–83	14–28
Top, central part (2)	0.8–1.6	6–14	9–17
i-side (3)	0.04–0.4	14–34	0.5–4
VPS coating (back side)			
Graphite substrate	<0.003	Up to 5	<0.003
e-side	0.6–1.2	C deposit not determined on the graphite substrate	0.01–0.1 over the whole area
Central part	0.03–0.3		
i-side	0.7–1.0		

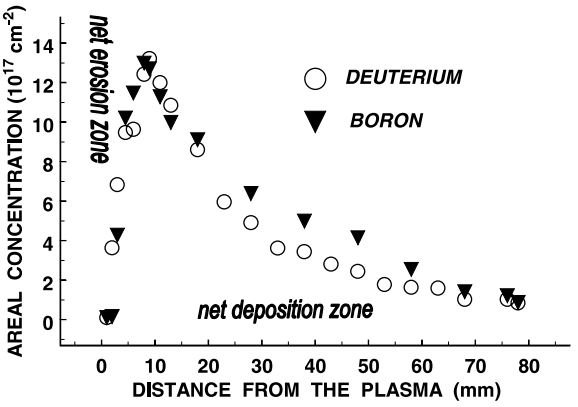

Fig. 2. Radial profiles of deuterium and boron on the side surface of the poloidal limiter.

observed on the divertor tiles of ASDEX-Upgrade where the power load (6 MW m^{-2} [10]) was evenly distributed over a larger area. The formation of micro-cracks on a few tiles only (out of some hundreds) has been reported.

3.2. B_4C coating

The appearance of the exposed B_4C coated limiter is shown in Fig. 3(a). In the areas of the highest heat loads, the coating is damaged (exfoliated and/or molten) but no layer detachment has occurred and no bare copper substrate is perceived. There are pits caused by arcing on the whole surface. Their shape and structure are shown in detail in Fig. 3(b). This type of damage has not been observed on sole W and C test limiters exposed under very similar conditions. The analyses were done along several lines in the toroidal (solid lines in Fig. 3(a)) and the poloidal (dashed lines) direction in order to recognize the D content in damaged and non-damaged zones, i.e. in areas of possibly different chemical composition. Plots in Fig. 4 show the deuterium distribution along the toroidal direction: one line crossing the exfoliated area (limiter center line, filled symbols) and the other one outside this area (open symbols). First of all, the deposition zones (≈20 mm wide), related to carbon transport and its co-deposition, are observed on far ends of the limiter. The D content in these zones amounts to $1-2\times10^{17}$ D atoms cm^{-2} and it is rather dependent on the exposure time than on the initial target composition, because the formation of such zones has also been observed on all other test limiters including sole tungsten and graphite. However, the fuel distribution in the central part of the B_4C coating is highly non-uniform. There are significant differences, by a factor of 8–10, in the amount of trapped fuel outside and inside the damaged areas: 5×10^{16} and 4.5×10^{17} cm^{-2}, respectively. The difference in fuel content between the zones is very sharp and, moreover, the depth distribution of

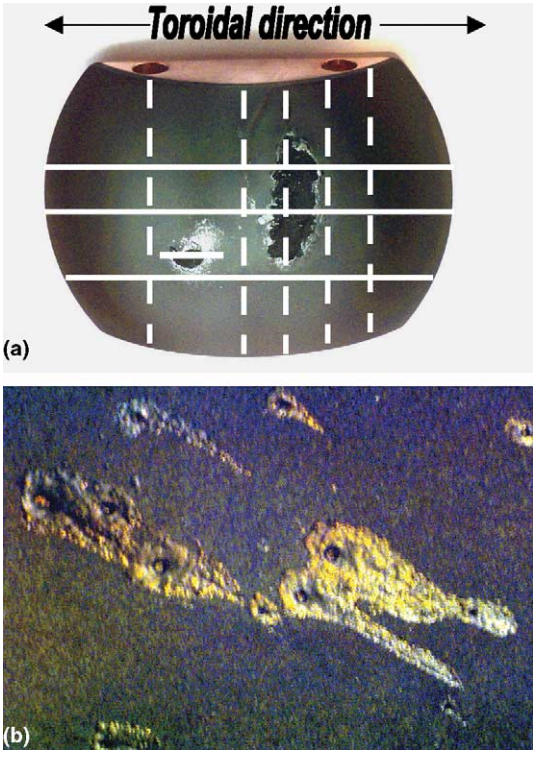

Fig. 3. B_4C coated test limiter after the exposure to the plasma. Dimensions of test limiters: projected length 120 mm (toroidal direction), projected width 60 mm (poloidal direction), radius of curvature 140 mm, height 45 mm, area of the plasma facing surface 100 cm^2. (a) An overview of the limiter surface with melted zones. The net of analysis scans is marked: solid lines in the toroidal direction and dashed lines in the poloidal one. (b) Arcing on the limiter surface.

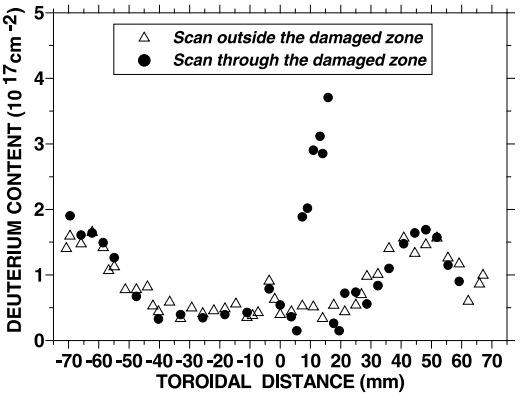

Fig. 4. Deuterium distribution and concentration, along the toroidal direction, on the exposed B_4C coated test limiter.

deuterium in the exfoliated zone is deeper (over 3 μm) than in the adjacent region (<0.5 μm). It gives a clear indication that the chemical composition of the zones

differs distinctly. Besides B, C and D the presence of copper and silicon is detected over the whole surface. The melted region contains bigger amount of Cu than observed on the rest of the surface but, nevertheless, Cu remains the minority species in comparison to B and C. While the Si presence is related to the machine siliconization, the Cu overlayer originates most probably from the transport of copper eroded of the sides of the limiter. The contribution of the arcing on the test specimen to the spread of copper cannot be excluded. The latter effect, however, is not considered as the major source because the plasma contamination by Cu was negligible.

The damage to the coating occurred at the surface temperature exceeding 1800 °C, as inferred from thermography ($T_m(B_4C) = 2460$ °C). One may suggest that the event stimulated chemical reactions and phase transition in the overheated topmost layer. Detailed analysis of the literature data [25,26] for Cu–B, Cu–C (and Cu–Si) systems shows that simple binary compounds, acetylenides or low-copper eutectic alloys can be excluded. Exact composition of compound(s) [Cu–B–C–Si] resulting from the high temperature reaction and material mixing on PFC cannot then conclusively be inferred. However, the mixture formed has high affinity towards the retention of deuterium. This feature should be taken into account when considering B_4C coated copper as a potential candidate material for PFC.

4. Comparison and conclusions

Fuel inventory was studied in four materials used as limiters at TEXTOR. The results obtained earlier for sole graphite and tungsten [3] are compared with those recent results for VPS coatings. Surface morphology in the topmost part (i.e. exposed to the highest power loads) of all the limiters is compared. The D-retention reaching 3.6×10^{17} cm^{-2} is observed on the VPS-W coating and it is mainly related with W, C and B mixing on the surface. Also molten parts of the B_4C coated specimen contain similar amount of trapped fuel. The D-retention in the non-damaged B_4C layer ($5–7 \times 10^{16}$ cm^{-2}) is therefore 1.5–2 times higher than that observed in sole graphite (3.5×10^{16} cm^{-2}) exposed under similar conditions. It is nearly two orders of magnitude bigger than that measured in sole tungsten ($<1 \times 10^{15}$ cm^{-2}). The results clearly show significant differences in fuel inventories between sole tungsten and carbon-containing materials. They also might indicate that no co-deposition of fuel (tritium inventory) should be expected in a device with PFC made only of tungsten.

Acknowledgements

We thank the TEXTOR team for kind co-operation. This work was partly carried out under the NFR contract F5102-20006021/2000 and a grant-in-aid for scientific research by the Ministry of Education, Culture and Science of Japan. The Wallenberg Foundation is highly acknowledged for funding the SEM–EDS equipment used in these studies.

References

[1] J.P. Coad et al., J. Nucl. Mater. 290–293 (2001) 224.
[2] G. Federici et al., J. Nucl. Mater. 266–269 (1999) 14.
[3] M. Rubel et al., J. Nucl. Mater. 283–287 (2000) 1089.
[4] M. Rubel et al., J. Nucl. Mater. 266–269 (1999) 1185.
[5] J.P. Coad, M. Rubel, C.H. Wu, J. Nucl. Mater. 241–243 (1997) 408.
[6] C.H. Skinner et al., J. Nucl. Mater. 290–293 (2001) 486.
[7] E. Vietzke, A.A. Haasz, in: W.O. Hofer, J. Roth (Eds.), Physical Processes of the interaction of Fusion Plasmas with Solids, Academic Press, 1996 (Chapter 4).
[8] A.A. Haasz et al., in: R.k. Janev (Ed.), Atomic and Plasma-Material Interaction Data for Fusion, 7A, IAEA, Vienna, 1998.
[9] W.R. Wampler et al., J. Nucl. Mater. 266–269 (1999) 217.
[10] H. Maier et al., J. Nucl. Mater. 258–263 (1998) 921.
[11] K. Krieger, H. Maier, R. Neu, ASDEX Upgrade Team, J. Nucl. Mater. 266–269 (1999) 207.
[12] R. Neu et al., J. Nucl. Mater. 290–293 (2001) 206.
[13] V. Philipps et al., J. Nucl. Mater. 258–263 (1998) 858.
[14] N. Noda, V. Philipps, R. Neu, J. Nucl. Mater. 241–243 (1997) 227.
[15] M. Rubel, T. Tanabe, V. Philipps, A. Huber, Phys. Scr. T 81 (1999) 61.
[16] A. Huber et al., Phys. Scr. T 91 (2001) 61.
[17] S. Kötterl et al., Phys. Scr. T 91 (2001) 117.
[18] A. Boscary et al., Phys. Scr. T 91 (2001) 90.
[19] T. Denner, K.F. Finken, G. Mank, N. Noda, Nucl. Fus. 39 (1999) 83.
[20] A. Pospieszczyk et al., J. Nucl. Mater. 290–293 (2001) 947.
[21] T. Tanabe et al., Fus. Eng. Des. 49–50 (2000) 355.
[22] R. Behrisch et al., J. Nucl. Mater. 145–147 (1987) 723.
[23] K. Tokunaga et al., in: N. Noda (Ed.), Proc. Japan–US Workshop on High Heat Flux Components and Plasma Surface Interactions for Next Fusion Devices, NIFS, Toki, 1998, 172.
[24] K. Tokunaga et al., J. Nucl. Mater. 266–269 (1999) 1224.
[25] H.J. Goldschmidt, Interstitial Alloys, Butterworths, London, pp. 296, 301, 322.
[26] Gmelin Handbuch der anorganischen Chemie, Kupfer, Verlag Chemie GmbH, Weinheim/Bergstrasse, vol. 60, 1961, pp. 625, 904.